AN OVERVIEW OF REAL TIME ULTRASOUND IMAGING MODALITIES

[1] KINITA B VANDARA, [2] DR. G.R.KULKARNI

[1] Research Scholar, Department of Electronics and Communication Engineering, Shri J.J.T.University, Vidyanagari, Jhunjhunu, Rajasthan
[2] Principal, C.U.Shah College Of Engineering And Technology, Wadhwan - 363030 Gujarat

kinitawandra.er@gmail.com, grkulkarni29264@rediffmail.com

ABSTRACT*: In this paper, an overview of medical Ultrasound imaging Modalities is presented. Thereafter, the physical phenomenon and detail process of signal capturing to image formation in Ultrasonography (USG) are presented. The paper deals with the methods and the measures that can be used in imaging technology. Also establish the structure of different noise models and artefacts associated with the respective medical modalities.*

Summary

In this paper a summary of the image formation process in Ultrasonography (USG) medical imaging modality have been presented. The most common noises, artefacts and distortions related with modality have been explored. The fundamentals of different artefacts, noises and other image degradation factors in respective modalities are briefly reviewed. The noise associated with medical Ultrasound images is depends on physics of modality. For the ultrasound images, speckle noise is the major affecting noise.

1. Ultrasonography (USG)

Ultrasound imaging application in medicine and other fields is enormous. It has several advantages over other medical imaging modalities. The use of ultrasound in diagnosis is well established because of its non-invasive nature, low cost, capability of forming real time imaging and continuing improvement in image quality. It is estimated that one out of every four medical diagnostic image studies in the world involves ultrasonic techniques. US waves are characterized by frequency above 20 KHz which is the upper limit of human hearing. In medical US applications, frequencies are used between 500 KHz and 30 MHz B-mode imaging is the most used modality in medical US. An US transducer which is placed onto the patient's skin over the imaged region sends an US pulse which travels along a beam into the tissue. Due to interfaces some of the US energy is reflected back to the transducer which converts it into echo signals. These signals are then sent into amplifiers and signal processing circuits in the imaging machine's hardware to form a 2-D image. This process of sending pulses launched in different directions is repeated in order to examine the whole region in the body. Thus, US imaging involves signals which are obtained by coherent summation of echo signals from scatterers in the tissue. In many cases volume quantification is important in assessing the progression of diseases and tracking progression of response to treatment. Thus, 3D ultrasound imaging has drawn great attention in recent years. Fig (1) shows a functional block diagram of an ultrasound imaging system. The construction of ultrasound B-mode image involves capturing the echo signal returned from tissue at the surface of piezoelectric crystal transducers. These transducers convert the ultrasonic RF mechanical wave into electrical signal. Convex ultrasound probes collect the echo from tissue in a radial form. Each group of transducers is simultaneously activated to look at a certain spatial direction from which they generate a raw line signal (stick) to be used later for raster image construction. These sticks are then demodulated and logarithmically compressed to reduce their dynamic range to suit the commercial display devices. The final Cartesian image is constructed from the sampled brushwood in a process called scan conversion. Speckle reduction techniques can be applied on envelope detected data, log compressed data or on scan converted data. However, slightly different results will be produced for each data. In the compression stage some useful information about the imaged object may be deteriorated or even lost. However, any processing which works with envelope detected data has more information at its disposal and preserves more useful information. Compared to processing the scan converted image, envelope detected data has fewer pixels and thus incurs lower computational cost. For optimum result envelope detected data processing is preferred because some information that lost after the compression stage cannot be recovered by working with logs compressed data or the scan converted image. However, the real time speckle reduction methods are applied on the scan converted image, since the scan converted image is always accessible where most commercial ultrasound systems do not output the envelope detected or log compressed data.

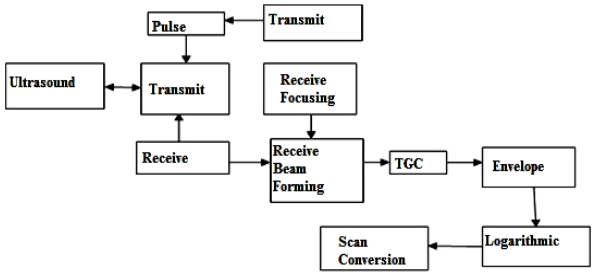

Figure 1 Block diagram of Ultrasound Imaging System

USG Basics

Sounds with a frequency above 20 kHz are called ultrasonic, since they occur at frequencies inaudible to the human ear. When emitted at short bursts, propagating through media, such as water, with low reflection coefficients and reflected by obstacles along their circulation path, the detection of the reflection, or echo, of the ultrasonic wave can help localize the obstacle.

2. Wave equation

As the ultrasonic wave propagates through the tissue, its energy and momentum are transferred to the tissue. No net transfer of mass occurs at any particular point in the medium unless this is induced by the momentum transfer. As the ultrasonic wave passes through the medium, the peak local pressure in the medium increases. The oscillations of the particles result to harmonic pressure variations within the medium and to a pressure wave that propagates through

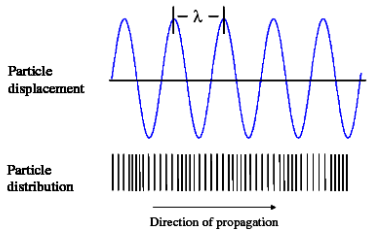

Figure 2 Particle displacement & Particle distribution for a travelling longitudinal wave

The direction of propagation is from left to right, namely the longitudinal (or, axial) direction. A shear wave can be created in the perpendicular direction, in which case the particles would also be moving in a direction orthogonal to the direction of propagation (not shown here). The medium as neighbouring particles move with as concerns to one another as shown in fig (2). the particles of the medium can move back and forth in a direction parallel (longitudinal wave) or perpendicular (transverse wave) to the travelling direction of the wave. Let's consider the first case. Assuming that a small volume of the medium that can be modelled as a non viscous fluid (no shear waves can be generated) is shown on figure 3, an applied force δF produces a displacement of u + δu *in* the x-position on the right-hand side of the small volume.

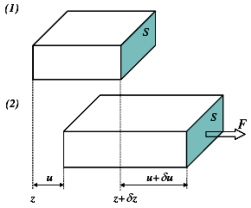

Figure 3 Small volume of the medium of impedance Z (1) at equilibrium and (2) undergoing oscillatory motion when an oscillatory force F is applied.

A gradient of force $\partial F/\partial z$ is thus generated across the element in question, and, assuming that the element is small enough so that the measured quantities within the medium are constant, it can be assumed as being linear, or:

$$\delta F = \frac{\partial F}{\partial z}\delta z \qquad \ldots 1$$

And according to hooke's Law,

$$F = KS\frac{\partial u}{\partial z'} \qquad \ldots 2$$

Where *K* is the adiabatic bulk modulus of the liquid and *S* is the area of the region on which the force is exerted. By taking the derivative of both sides of equation (2) with respect to *z* and following Newton's Second Law, from equation (1) we obtain the so-called "wave equation":

$$\frac{\partial^2 u}{\partial z^2} - \frac{1}{C^2}\frac{\partial^2 u}{\partial t^2} = 0 \quad \text{... 3}$$

Where *c* is the speed of sound given by $c = \sqrt{\frac{K}{\rho}} = \sqrt{\frac{1}{\rho k}}$ and ρ is the density of the medium and the compressibility of the medium is denoted by ρk . Equation (3) relates the second differential of the participle displacement with respect to distance to the acceleration of a simple harmonic oscillator. For the shear wave derivation of this equation please refer to Wells1 or Kinsley and Frey2 among others.

The solution of the wave equation is given by a function *u*, where:

$$u = u\,(ct - z) \quad \text{... 4}$$

An appropriate choice of function for *u* in Eq. 4 can be:

$$u\,(t, z) = u_0 \exp[jk(ct - z)] \quad \text{... 5}$$

Where, k is the wave number and equal to $2\pi/\lambda$ with λ denoting the wavelength Fig (5).

3. Impedance, power and reflection

The pressure wave that results from the displacement generated and given by Equation (5) is given by:

$$p\,(t, z) = p0 \exp[jk(ct - z)] \quad \text{... 6}$$

Where p_0 is the pressure wave amplitude and *j* is equal to $\sqrt{-1}$. The particle speed and the resulting pressure wave are related through the following relationship:

$$u = P/Z \quad \text{... 7}$$

Where Z is the acoustic impedance defined as the ratio of the acoustic pressure wave at a point in the medium to the speed of the particle at the same point. The impedance is thus characteristic of the medium and given by:

$$Z = \rho c. \quad \text{... 8}$$

The average flow of energy through a unit area in the medium perpendicular to the direction of propagation is known as the acoustic wave intensity. By following that definition, the intensity can be found equal to:

$$I = \frac{p^2{}_0}{2z} \quad \text{... 9}$$

And usually, I measured in units of mW/cm^2 in diagnostic ultrasound. A first step into understanding the generation of ultrasound images is to follow the interaction of the propagating wave with the tissue. Thanks to the varying mean acoustic properties of tissues, a wave transmitted into the tissue will get partly reflected at areas where the properties of the tissue and, thus its impendence, are changing. These areas constitute a so called "impedance mismatch" shown in fig (4)

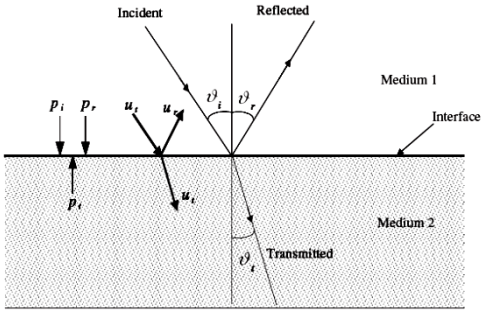

Figure 4 an incident wave at an impedance mismatch (interface)

A reflected and a transmitted wave with certain velocities and pressure amplitudes are created ensuring continuity at the boundary.

The reflection coefficient *R* of the pressure wave at an incidence angle of *ϑi is* given by:

$$R = pr/pi = Z_2\cos\vartheta t - Z_1\cos\vartheta i \,/ Z_2\cos\vartheta t + Z_1\cos\vartheta i \quad \text{... 10}$$

Where *ϑt* is the angle of the transmitted wave Fig (4) also related to the incidence angle through Snell's Law:

$$\lambda 1 \cos \vartheta i = \lambda 2 \cos \vartheta t \quad \text{... 11}$$

Where $\lambda 1$ and $\lambda 2$ are the wavelengths of the waves in medium 1 and 2, respectively, and related to the speeds in the two media through:

$$c = \lambda f \quad \text{... 12}$$

Where, *the* frequency of the propagating wave is denoted by f. As Fig (4) also shows, the wave impingent upon the impedance mismatch also generates a transmitted wave, i.e. a wave that propagates through. The transmission coefficient is defined as:

$$T = pt/pi = 2Z_2 \cos \vartheta i \,/ Z_2 \cos \vartheta i + Z_1 \cos \vartheta t \quad \text{... 13}$$

According to the parameters impedance and speed of sound of air, water and certain tissues, the reflection coefficient at a fat-air interface is equal to −99.94% showing that virtually the entire energy incident on the interface is reflected back in tissues such as the lung.
A more realistic example found in the human body is the muscle-bone interface, where the reflection coefficients 49.25%, demonstrating the challenges encountered when using ultrasound for the investigation of bone structure. On The other hand, given the overall similar acoustic properties between different soft tissues, the reflection coefficient is too low when used to differentiate between different soft tissue structures ranging only between −10% and 0. The values mentioned above determine both the interpretation of ultrasound images, or sonograms, as well as the design of transducers, as discussed in the sections below.

4. Tissue scattering

In fact, tissues are constituted by cells and groups of cells that serve as complex boundaries to the propagating wave. As the wave propagates through all these complex structures, reflected and transmitted waves are generated at each one of these interfaces dependent on the local density, compressibility and absorption of the tissue. The groups of cells are called "scatterers" as they scatter acoustic energy. The backscattered field, or what is "scattered back" to the transducer, is used to generate the ultrasound image. In fact, the backscattered echoes are usually coherent and can be used as "signatures" of tissues that are e.g. in motion or under compression, as applied in elasticity imaging methods. An example of such an ultrasound image can be seen in fig (5). The capsule of the prostate is shown to have a strong echo, mainly due to the high impedance mismatch between the surrounding medium, gel in this case, and the prostate capsule. However, the remaining area of the prostate is depicted as a grainy region surrounding the fluid filled area of the urethra (dark or low scattering, area in the middle of the prostate).This grainy appearance.

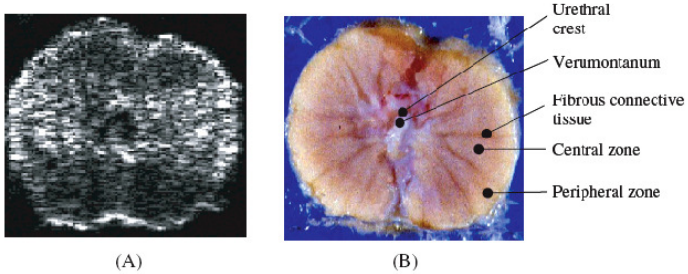

Figure 5 Sonogram of (A) an in vitro canine prostate and (B) its corresponding anatomy

At the same plane as that scanned Called "speckle". Speckle is produced by the constructive and destructive interference of the scattered signals from structures smaller than the wavelength; hence, the appearance of bright and dark echoes, respectively. So, speckle does not necessarily relate to a particular structure in the tissue. Given its statistical significance, in its simplest representation, the amplitude of speckle has been represented as having a Gaussian distribution with a certain mean and variance. In fact, these same parameters have been used to indicate the signal to- noise ratio for speckle noise in ultrasound images.

5. Attenuation

As the ultrasound wave propagates inside the tissue, it undergoes a loss of power dependent on the distance travelled in the tissue. Attenuation of the ultrasonic signal can be attributed to a variety of factors, such as divergence of the wave front, reflection at planar interfaces, scattering from irregularities or point scatterers and absorption of the wave energy. In this section, we will concentrate on the latter, being the strongest factor in soft (other than lung) tissues. In this case, the absorption of the wave's energy leads to heat increase. The actual cause of absorption is still relatively unknown but simple models have been developed to demonstrate the dependence of the resulting wave pressure amplitude decrease in conjunction with the viscosity of tissues.
By not going into detail concerning the derivations of such a relationship, an explanation of the phenomenon is provided here. Let's consider a fluid with a certain viscosity that provides a certain resistance to a wave propagating through its different layers. In order to overcome the resistance, a certain force per unit area or, pressure, needs to be applied that is proportional to the shear viscosity of the fluid η as well as the spatial gradient of the velocity or:

$$p \propto \eta \frac{\partial u}{\partial z} \qquad \ldots 14$$

Equation (14) shows that a fluid with higher viscosity will require higher force to experience the same velocity gradient compared to a less viscous fluid. By considering equation (2) and (14), an extra term can be added to the wave equation that involves both the viscosity and compressibility of the medium, or:

$$\frac{\partial^2 u}{\partial z^2} + (4\eta + \xi)k\frac{\partial^3 u}{\partial z^2\,\partial t} - \frac{1}{C^2}\frac{\partial^2 u}{\partial t^2} = 0 \qquad \ldots 15$$

Where, ξ denotes the dynamic coefficient of compression viscosity. The solution to this equation is given by:

$$u(t, z) = u_0 \exp(-\alpha z) \exp[jk(ct - z)] \quad \ldots 16$$

Where α is the attenuation coefficient also given by (for $\alpha \ll k$):

$$\alpha = \frac{(4\eta+\xi)K^2}{2\rho c} \quad \ldots 17$$

From equation (16), the effect of attenuation on the amplitude of the wave is clearly depicted Figure 6. An exponential decay on the envelope of the pressure wave highly dependent on the distance results from the tissue attenuation. The intensity of the wave will decrease at twice the rate, given that from equation (9).

$$I(t, z) = \rho_0{}^2 / Z \exp(-2\alpha z) \exp[2jk(ct - z)] \quad \ldots 18$$

Or, the average intensity is equal to:

$$I = I_0 \exp(-2\alpha z) \quad \ldots 19$$

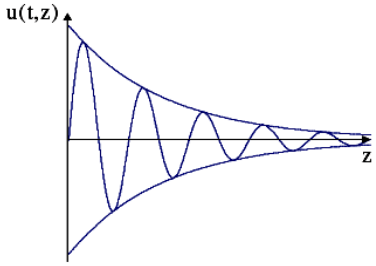

Figure 6 the Attenuated Wave

Another important effect that the tissue attenuation can have on the propagating wave is a frequency shift. This is because a more complex form for the attenuation α is:

$$\alpha = \beta_0 + \beta_1 f \quad \ldots 20$$

Where $\beta 0$ and $\beta 1$ are the frequency-independent and frequency dependent attenuation coefficients.

In fact, the frequency-dependent term is the largest source of attenuation and increases linearly with frequency. As a result, the spectrum of the received signal changes as the pulse propagates through the tissue in such a way that a shift to smaller frequencies, or downshift, occurs. In addition, the downshift is dependent on the bandwidth of the pulse propagating in the tissue and the mean frequency of a spectrum can be given by:

$$f = f_0 - (\beta_1 B^2 f^2{}_0) z \quad \ldots 21$$

Where, f_0 and B denote the centre frequency and bandwidth of the pulse. Thus, according to equation (21), the downshift due to attenuation depends on the tissue frequency-dependent attenuation coefficient, and the pulse centre frequency and bandwidth. A graph showing the typical values of frequency-dependent attenuation coefficients (measured in dB/cm/MHz) in the biological tissue is given in fig (7).

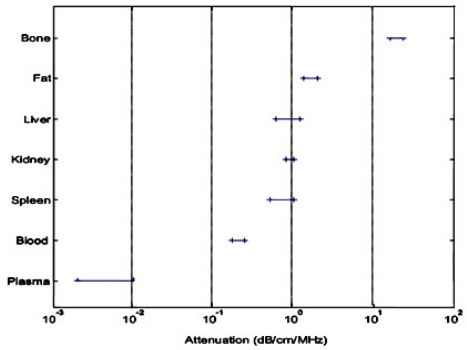

Figure 7 Attenuation values of certain fluids and soft tissues

6. Transducers

The pressure wave is generated using an ultrasound transducer, which is typically a piezoelectric material. "Piezoelectric" denotes the particular property of certain crystal polymers of transmitting a pressure ("piezo" means "to press" in Greek) wave generated when an electrical potential is applied across the material. Most importantly, since this piezoelectric effect is reversible, i.e. a piezoelectric crystal will convert an impinging pressure wave to an electric potential, the same as transducer can also be utilize as a receiver. Such crystalline or semi crystalline polymers are the poly vinylidene fluoride, quartz, barium titanate and lead zirconium titanate.

A single-element ultrasound transducer is shown in fig (8). Dependent upon it thickness (l) and propagation speed (c), the piezoelectric material has a resonance frequency given by:

$$f_0 = \frac{C}{2l} \quad \ldots 22$$

The speed in the PZT material is around 4000 ms^{-1}, so for a 5MHz transducer, the thickness should be 0.4mm thick. The matching layer is usually coated onto the piezoelectric crystal in order to minimize the impedance mismatch between the crystal and the skin surface and, thus, maximize the transmission coefficient equation (13). In order to overcome the aforementioned impedance mismatch, the ideal impedance Zm and thickness *dm* of the matching layer are respectively given by:

$$Zm = \sqrt{Z_T Z} \quad \text{and} \qquad \ldots 23$$

$$Dm = \frac{\lambda}{4} \qquad \ldots 24$$

Where, Z_T is the transducer impedance and Z the impedance of the medium. The backing layers behind the piezoelectric crystal are used in order to increase the bandwidth and the energy output. If the backing layer contains air, then the air-crystal interface yields a maximum reflection coefficient given the high impedance mismatch. Another by-product of an air-backed crystal element is that the crystal remains relatively un-damped, i.e. the signal transmitted will have a low bandwidth and a longer duration.

On the other hand, the axial resolution of the transducer depends on the signal duration, or pulse width, transmitted. As a result, there are tradeoffs between transmitted power and resolution of an ultrasound system. Depending on the application, different backing layers are therefore used. Air-backed transducers are used in continuous wave and ultrasound therapy applications. Heavily-backed transducers are utilized in order to obtain high resolution, e.g. for high quality imaging at the expense of lower sensitivity and reduced Penetration.

Coded-excitation techniques have recently been successfully applied to circumvent such tradeoffs.

For imaging purposes, an assembly of elements such as that in fig (8) is usually used and called an "array" of such elements. In an array, the elements are stacked next to each other at a distance equal to less than a wavelength for the minimum interference and reduced grating lobes. The linear array has the simplest geometry.

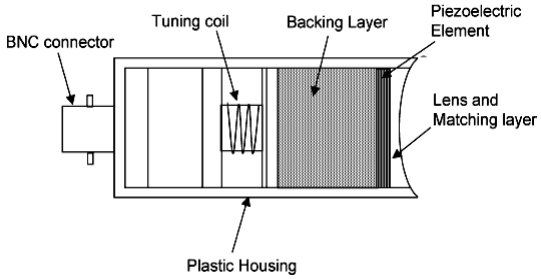

Figure 8 Typical construction of a single-element transducer.

It selects the region of interest by firing elements above that region. The beam can then be moved on a line by firing groups of adjacent elements and then the rectangular image obtained is formed by combining the received signals by all the elements. A curved array is used when the transducer is smaller than the area scanned. A phased array can be used to change the "phase" or delay between the fired elements and thus achieve steering of the beam. The phased array is usually the choice for cardiovascular exams, when the window between the ribs allows for a very small transducer to image the whole heart. Focusing and steering can both be achieved by modifying the profile of firing delays between elements fig (9).

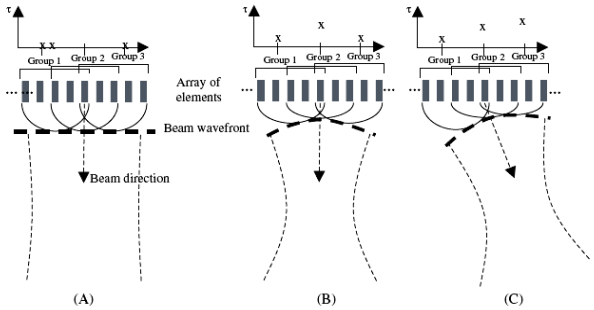

Figure 9 Electronic beam forming (A) beam forming, (B) focusing and (C) focusing and beam steering as achieved in phased arrays.

The time delay between the firings of different elements is denoted here by τ

7. Ultrasonic instrumentation

Figure 10 shows a block diagram of the different steps that are used in order to acquire process and display the received signal from the tissue.

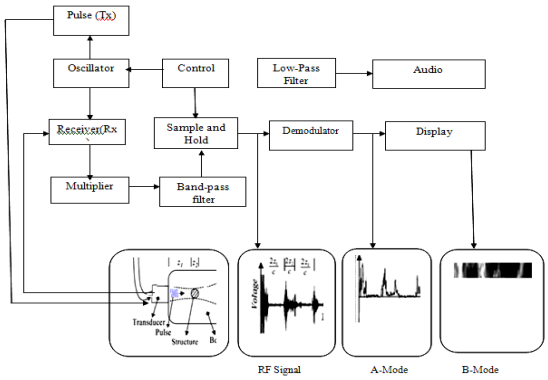

Figure 10 Block diagram of a pulsed-wave system and the resulting signal or image at three different steps.

i. Transducer frequency

In ultrasound imaging, a pulse of a given duration, frequency and bandwidth is first transmitted. As mentioned before, a trade off between penetration (or, low attenuation) and resolution exists

Therefore, the chosen frequency will depend on the application. Usually, for deeper-organs, such as the heart, the uterus and the liver, the frequencies are restricted in the range of 3 MHz–5MHz while for more superficial structures, such as the thyroid, the breast, the testis and applications on infants, a wider range of 4 MHz–10MHz is applied. Finally, for ocular applications, a range of 7 MHz–25MHz is determined by the low attenuation, low depth and higher resolution required. The pulse is usually a few cycles of that frequency long (usually 3–4 cycles) so as to ensure high resolution, and is generated by the transmitter through a voltage step sinusoidal function at a voltage amplitude (100V–500 V) and a frequency equal to that of the resonance frequency of the transducer elements.

For static structures, a single pulse or multiple pulses (usually used for averaging later) could be used at an arbitrary frequency. However, for moving structures, such as blood, liver and the heart, a fundamental limit on the maximum pulse repetition frequency (PRF) is set by the maximum depth of the structure, or PRF (kHz) = c/2Dmax. Typically, the PRF is in the range of 1 kHz–3 kHz.

ii. RF Amplifier

The received signal needs to be initially amplified so as to guarantee a good signal-to-noise ratio. At the same time, the input of the amplifier should be devoid of the high voltage pulse in order to protect the circuits but also maintain its low noise and high gain. A typical dynamic range expected at the output is on the order of 70 dB–80 dB.

iii. Time-gain compensation (TGC)

The attenuation is unavoidable as the wave travels through the medium and it increases with depth. In order to avoid artificial darkening of deeper structures as a result, a voltage controlled attenuator is usually employed, where a control voltage is utilized to manually adjust the system gain accordingly after reception of an initial scan .Algorithmic voltage ramp is usually applied that compensates for a mean attenuation level with depth. The dynamic range becomes further reduced to 40 dB–50 dB.

Iv.Compression amplifier

The signals will ultimately be displayed as a gray scale on a cathode ray tube (CRT), where the dynamic range is typically only 20 dB– 30 dB. To this purpose, an amplifier with a logarithmic response is utilized.

8. Ultrasound mode

Ultrasonic imaging is usually known as echography or sonography, depending on which side of the Atlantic Ocean one is scanning from. As mentioned earlier, the signal acquired by the scanner can be processed and displayed in several different fashions. In this section, the most typical and routinely used ones are discussed.

i. A-mode

Since the image is a gray scale picture, the amplitude of the signal is displayed. For this, the envelopes of the RF signal needs to be calculated. This is, for example, achieved by applying the Hilbert transforms. The resulting signal is called a detected A-scan, A-line or *A-mode scan* (A- for Amplitude).

ii. B-mode

When the received A-scans are spatially combined after acquisition using either a mechanically moved transducer or the previously mentioned arrays and used to brightness-modulate the display in a 2D format, the brightness or B-mode is created, which has a true Top: B-scan of an abdominal aorta in a mouse at 30 MHz; Bottom: M-mode image over several cardiac cycles taken along the dashed line in the B-scan. Image format and is by far the most widely used diagnostic ultrasound mode. By default, sonogram or echogram refers to B-mode.

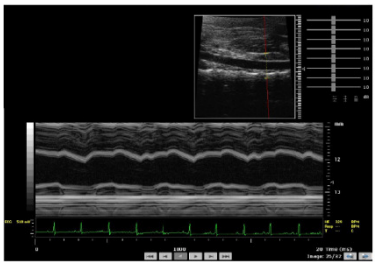

Figure 11 Longitudinal B-mode image of an abdominal aorta

One of the biggest advantages of ultrasound scanning is real-time scanning and this is achieved due to the shallow depth of scanning in most tissues and the high speed of sound. The frame rate is usually on the order of 30 Hz–100 Hz (while in the M-mode version it can be as fast the PRF itself, see below). The frame rate is limited by the number of A-mode scans acquired, *NA*, and the maximum depth,
I.e. the maximum frame rate is given by PRF = c/2Dmax × NA.

iii. M-mode

Another way of displaying the A-scans is in function of time, especially in cases where tissue motion needs to be monitored and analyzed such as the case of heart valves or other cardiac structures. In the case of figure 25, only one A-scan from a particular tissue structure is displayed in brightness mode and followed in time, called motion or M-mode scan. A depth-time display is then generated. A typical application of the M-mode display is used in the examination of heart valve leaflets motion and Doppler display.

9. Artefacts in Ultrasound Images

Artefacts refer to something seen on the ultrasound image that does not exist in reality. An artefact can be helpful interpreting the image or it can confuse the examiner. Several commonly encountered artefacts are mentioned below.

i. Attenuation Artefacts:

- *Shadowing:*

This artefact is caused by partial or total reflection or absorption of the sound energy. A much weaker signal returns from behind a strong reflector (air) or sound-absorbing structure (gallstone, kidney stone, bone, fig (12).

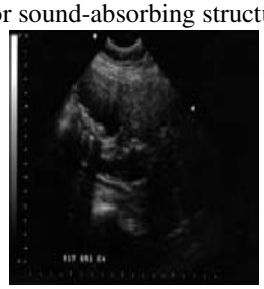

Figure 12 Attenuation (shadowing) artefact caused by gallstones

- *Posterior Enhancement:*

In posterior enhancement, the area behind an echo-weak or echo-free structure appears brighter (more echogenic) than its surrounding structures. This occurs because neighbouring signals had to pass through more attenuating structures and return with weaker echoes, Fig (13).

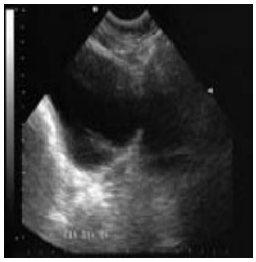

Figure 13 Posterior enhancements, side lobe and mirror artefact.

- *Edge Shadowing:*

The lateral edge shadow is a thin acoustic shadow that appears behind edges of cystic structures. Sound waves encountering a cystic wall or a curved surface at a tangential angle are scattered and refracted, leading to energy loss and the formation of a shadow.

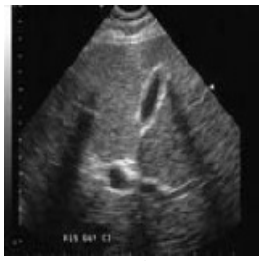

Figure 14: Edge artefact.

ii. Propagation Artefacts:

- *Reverberation:*

Reverberation occurs when sound encounters two highly reflective layers. The sound is bounced back and forth between the two layers before travelling back. The probe will detect a prolonged travelling time and assume a longer travelling distance and display additional 'reverberated' images in a deeper tissue layer Fig (15).

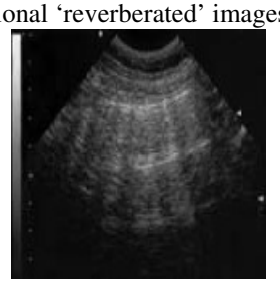

Figure 15 Reverberation artefacts.

- *Comet Tail:*

A comet tail artefact is similar to reverberation. It is produced by the front and back of a very strong reflector (air bubble, BB gun pellet). The reverberations are spaced very narrowly and blend into a small band, Fig (16).

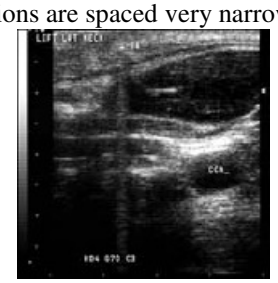

Figure 16 Comet tail artefacts

- *Mirror Imaging:*

If a structure is located close to a highly reflective interface (such as the diaphragm), it is detected and displayed in its normal position. However, the strong reflector causes additional sound waves to bend towards the neighbouring anatomy, from where they are bounced back towards the strong reflector and return to the transducer. These sound waves have a longer travel time and are perceived as an additional anatomic structure. The image is duplicated on the other side of the strong reflector, fig (17).

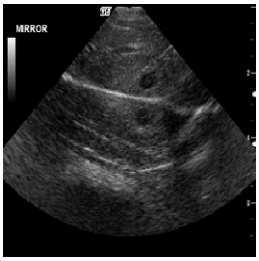

Figure 17 Mirror Imaging artefacts

iii. Miscellaneous Artefacts:

- *Ring Down:*

The artefact is caused by a resonance phenomenon from a collection of gas bubbles. A continuous emission of sound occurs from the 'resonating' structure causing a long and uninterrupted echo. It appears very similar to the comet tail artefact.

- *Side Lobe:*

This artefact is caused by low energy 'side lobes' of the main ultrasound beam. When an echo from such a side lobe beam becomes strong enough and returns to the receiver, it is 'assigned' to the main beam and displayed at a false location. Side-lobe artefacts are usually seen in hypo echoic or echo-free structures and appear as bright and rounded lines, fig (18).

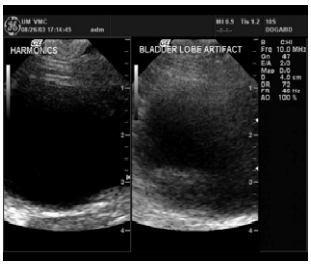

Figure 18 Side Lobe artefacts

10. Noises in Ultrasound Images

Ultrasound images are also degraded by image independent noise like in CT and MRI modalities. But speckle noise is the dominant factor for all ultrasound images. Speckle noise is defined as multiplicative noise and having a granular pattern. It is the inherent property of ultrasound images. The nature of the speckle pattern can be categorized into one of three classes according to the number of scatterers per resolution cell or the so called scattered number density, in addition to their spatial distribution and the characteristics of the imaging system itself. The FFS pattern occurs when many fine randomly distributed scattering sites exist within the pledge cell of the pulse-echo system. In this case, the amplitude of the backscattered signal can be modelled as a Rayleigh distributed random variable with a constant SNR of 1.9 Under such conditions, the textural features of the speckle pattern represent a random variable signature of the imaging instrument and its point spread function. Blood cells are classic examples of this type of scatterers. None randomly distributed with long-range order. It contributes a coherent backscattered intensity that is in itself spatially varying. Due to the connection between scatterers and the effective number of scatterers is finite. None randomly distributed with short-range order. Examples of this type consist of organ surfaces and blood vessels. When a spatially invariant coherent structure is present within the random scattered region, the probability density function (PDF) of the backscattered signals becomes close to the Rician distribution.

i. Speckle Noise

Another common form of noise is data dropout noise generally referred to as speckle noise. It is not a noise in an image but noise-like variation in contrast. This noise occurs due to errors in data transmission. This kind of noise affects the medical images. The corrupted pixels are either set to the maximum value, which is incredible similar to a flurry in image or have single bits flipped over. Speckle noise has the characteristic of multiplicative noise. Speckle noise follows a gamma distribution. Unwanted data which may reduce the contrast deteriorating the shape or size of objects in the image and blurring of edges or dilution of fine details in the image may be termed as noise. It may be due to one or more of the following reasons.

- Physical nature of the system

- Shortcomings of image acquisition devices
- Image developing mechanism
- Due to environment.

Mathematically there are two basic models of Noise; additive and multiplicative. Additive noise is systematic in nature and can be easily modelled and hence removed or reduced easily. Whereas multiplicative noise is image dependent, complex to model and hence difficult to reduce. When multiplicative noise caused by the de-phased echoes from the scatter appears, it is called "Speckle Noise". Although it appears as noise but it contains useful information. Speckle may appear distinct in different imaging systems but it is always manifested in a granular pattern due to image formation in coherent waves. Speckle is the result of the diffuse scattering, which occurs when RF pulse randomly interferes with the small particles. Speckle is an inherent property of medical images, and it is modelled as spatial correlated multiplicative noise. In most cases, it is considered a contaminating factor that severely degrades image quality. To improve image analysis, speckle reduction is generally used for visualization enhancement. Most speckle filters are developed for enhancing visualization of speckle images.

ii. Modal of Speckle Noise

Speckle is a random, deterministic, interference pattern in an image formed with coherent radiation of a medium containing several sub-resolution scatterers. Speckle has a negative impact on ultrasound imaging. The presence of speckle noise in images shows a reduction of lesion delectability. This radical reduction in contrast resolution is responsible for the poorer effective resolution of ultrasound compared to x-ray and MRI. Presence of speckle noise prevents Automatic Target Recognition (ATR) and texture analysis algorithm to perform efficiently and gives the image a grainy appearance. Hence, despeckling is considered as a critical pre-processing step in medical imaging systems. Speckle noise follows a gamma distribution and is given as

$$F(g) = \frac{g^{\alpha-1}}{(\alpha-1)!a^{\alpha}} e^{-\frac{g}{a}} \quad \text{... (25)}$$

Where a^{α} the variance and g is is the gray level. On an image, speckle noise (with variance 0.05) looks as shown in Fig (19a) and the corresponding gamma distribution is given in Fig (19b).

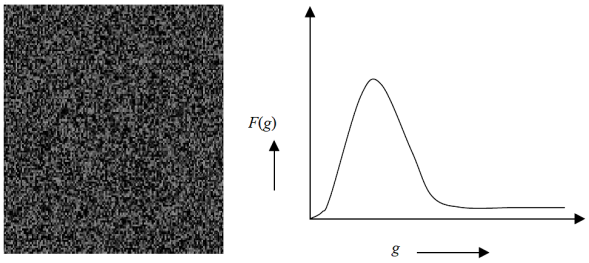

(a) Speckle Noise (b) Gamma Distribution

Figure 19 Speckle Noise and Distribution

iii. Mathematical Modal of speckle noise

An inherent characteristic of ultrasound imaging is the presence of speckle noise. Speckle noise is a random and deterministic in an image. Speckle has negative impact on ultrasound imaging, Radical reduction in contrast resolution may be responsible for the poor effective resolution of ultrasound as compared to MRI. In case of medical literatures, speckle noise is also known as texture. Generalized model of the speckle is represented as,

$$g(n,m) = f(n,m) * u(n,m) + \zeta(n,m) \quad \text{…(26)}$$

Where, g(n,m) is the observed image, u(n,m) is the multiplicative component and $\zeta(n,m)$ is the additive component of the speckle noise. Here n and m denotes the axial and lateral indices of the image sample. For the ultrasound imaging, only multiplicative component of the noise is to be considered and additive component of the noise is to be ignored. Hence, equation (1) can be modified as;

$$g(n,m) = f(n,m) * u(n,m) + \zeta(n,m) - \zeta(n,m)$$

Therefore,

$$g(n,m) = f(n,m) * u(n,m) \quad \text{…(27)}$$

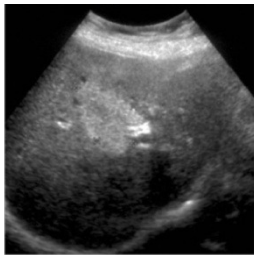

Original image

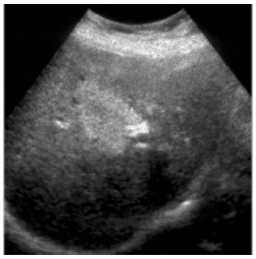

Noisy with Noise variance (0.02)

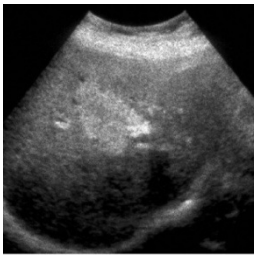

Noisy with Noise variance (0.05)

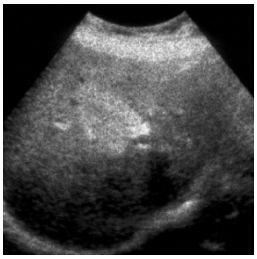

Noisy with Noise variance (0.1)

Figure 20 Ultrasound Image with Speckle Noise

Bibliography

1. Rafael C. Gonzalez and Richard E. Woods, "Digital Image Processing", Prentice-Hall, Inc., 2002.
2. Huiyu, Jiahua Wu and jianguo Zhang, "Digital Image Processing Part-1", Ventus Publishing ApS, 2010.
3. Isaac N Bankman, "Handbook of Medical Imaging Processing and Analysis", Academic Press, A Harcourt Science and Technology Company 2000.
4. Jasjit S. Suri, David C. Wilson and Swami Laxminarayan, "Handbook of Biomedical Image Analysis" Kluwer Academic / Plenum Publishers, 2005.
5. Geoff Dougherty, "Digital Image Processing for Medical Applications", Cambridge Press, 2009.
6. William R. Hendee and E. Russell Ritenour, "Medical Imaging Physics", Wiley-Lis, Inc.,2002.
7. Atam P Dhawan, H K Huang and Dae-Shik Kim, "Principles And Advanced Methods In Medical Imaging And Image Analysis", World Scientific Publishing Co. Pte. Ltd. 2008.
8. CiiT International Journal of Digital Image Processing Print: ISSN 0974 – 9691 & Online: ISSN 0974 – 9586.
9. Christos P. Loizou and Constantinos S. Pattichis," Despeckle Filtering Algorithms and Software for Ultrasound Imaging", Copyright © 2008 by Morgan & Claypool.
10. S.Kalaivani Narayanan and R.S.D.Wahidabanu, "A View on Despeckling in Ultrasound Imaging", International Journal of Signal Processing, Vol. 2, No.3, September 2009.
11. Jing Wang, Zhengrong Liang, Hongbing Lu, "Multiscale Penalized Weighted Least- squares Sinogram Restoration for Low-Dose X-Ray Computed Tomography", Engineering in Medicine and Biology Society, 2006, 28th Annual International Conference of the IEEE, pp.: 3282 – 3285.
12. Physics and Technical Facts for the Beginner http://www.sonoguide.com/physics.html 7] American College of Emergency Physicians,
13. Dikendra Verma, Sanjay Mathur, "Image De-noising Based on Averaging of Wavelet Transformed Images", International Journal of Engineering Research and Applications (IJERA) ISSN: 2248-9622, Vol. 2, Issue 5, September- October 2012, pp.2112-2119.
14. R. Eveline Pregitha,Dr. V. Jegathesan and C. Ebbie Selvakumar, "Speckle Noise Reduction in Ultrasound Fetal Images Using edge preserving Adaptive Shock Filter", International Journal of Scientific and Research Publications, Volume 2, Issue 3, March 2012 1 ISSN 2250-3153.
15. S.Kalaivani Narayanan1 , Dr.R.S.D.Wahidabanu, "Despeckling of Ultrasound Imaging using Media Regularized Coupled Pde, ACEEE Int. J. on Control System and Instrumentation, Vol. 02, No. 02, June 2011
16. http://dukemil.bme.duke.edu/Ultrasound/k-space/node5.html
17. Jing Wang, Zhengrong Liang, Hongbing Lu, "Multiscale Penalized Weighted Least- squares Sinogram Restoration for Low-Dose X-Ray Computed Tomography", Engineering in Medicine and Biology Society, 2006, 28th Annual International Conference of the IEEE, pp.: 3282 – 3285.
18. Milindkumar V. Sarode, Prashant R. Deshmukh**,"**Reduction of Speckle Noise and Image Enhancement of Images Using Filtering Technique" International Journal of Advancements in Technology http://ijict.org/ ISSN 0976-4860.